SAND2022-4928R

ENG 572 Interim Report

Jeffrey Zhao

June 19, 2020

Introduction

Sandia National Laboratories is a Federally Funded Research and Development Center (FFRDC) founded in 1949 with the mission of developing and testing the non-nuclear components of nuclear weapons. Sandia has since been involved with numerous projects to support the Department of Defense's (DOE) National Nuclear Security Administration (NNSA). One such set of projects has been implementing over-the-road transportation security enhancements. Under this program, Sandia National Laboratories (SNL) has worked to develop interface compatibility modifications for existing shipping configurations. This summer I will be working with a line of trailers that have been used to transport high asset cargo. These vehicles have successfully traveled millions of miles without any accidents over the course of 15 years.

The primary motivation for the work that I will complete this summer is to provide support for existing electronic communication technologies implemented at SNL. As part of an ongoing project to implement modifications to a trailer system, I will focus primarily on the characterization and testing of thermal electric coolers (TEC). Within the scope of the trailer project, these devices provide temperature control for lasers used on optical communication boards (OCB).

Literature Review of Technology

Thermoelectric materials have been heavily researched in the past few decades in response to their ability to convert temperature to voltage and vice versa. These materials have applications in alternative energy technologies as they are most commonly used to convert waste heat into electrical energy. Other applications include small, localized cooling in infrared detectors and computers, which have been quoted to produce speed gains ranging from 30-200% if integrated correctly with CMOS technology [1]. The focus of this paper will be to discuss a subset of such applications, i.e., thermoelectric coolers, otherwise known as Peltier coolers.

Operation

A thermoelectric cooler is a device that relies on the heating/cooling nature of a thermocouple. This component is created by combining two different metals at two junctions on either end as seen in Figure 1. The "cold" junction is generally used as the reference temperature and the "hot" junction is used to measure an external heat source.

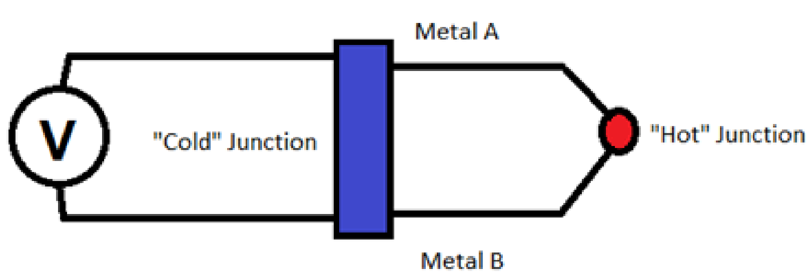

Fig. 1. Typical setup for characterizing thermocouples

The device can produce a thermal electromotive force (EMF) in response to a temperature differential applied between the junctions in an occurrence known as the Seebeck effect. Named after Thomas Johann Seebeck, the effect describes the physical phenomena whereby an electrical potential (∇V) is produced proportional to the temperature gradient (∇T). It can be described empirically as:

$$\nabla V = -S\nabla T \tag{1}$$

Where S, the Seebeck coefficient (otherwise called thermopower), is typically in the range of a few μV/K for commonly used conductive metals such as copper, silver, and gold [10]. A related effect known as the Peltier effect, which was discovered a few years later, describes the process in which an electric current passing through the junction of two dissimilar materials creates a temperature differential between the two ends dependent on the direction of current flow. This can be explained primarily by the difference in Fermi energies between the two junctions; however, effects such as the Hall, Ettingshausen, and Nernst play roles as well [2]. Combining the two effects yields the equation:

$$Qp = \Pi I \tag{2}$$

where Q_p is the Peltier heat emitted or evolved per unit time and Π is the Peltier coefficient $\Pi = ST$.

By placing several thermocouples in series or parallel, one can create a thermopile. These devices operate under the idea that current will flow along the temperature gradient. Within a solid-state component such as Figure 2, electric current circulates through the device to draw heat from one end and evolve it at another.

Sandia National Laboratories is a multimission laboratory managed and operated by National Technology & Engineering Solutions of Sandia, LLC, a wholly owned subsidiary of Honeywell International Inc., for the U.S. Department of Energy's National Nuclear Security Administration under contract DE-NA0003525. SAND2019-XXXX X

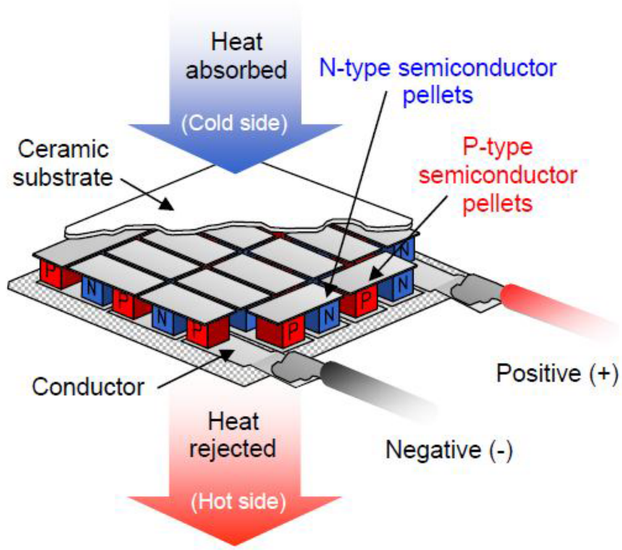

Fig. 2. Typical layout of semiconductor thermoelectric cooler using array of thermocouples [3]

Qualification of Thermoelectric Performance

A common characterization for the merit of a TE material is as follows:

$$ZT = \frac{S^2 T}{\rho\kappa} \quad (3)$$

where ρ is the electrical resistivity and κ is the thermal conductivity, and ZT is a dimensionless quantity known as the figure-of-merit. Although Z and ZT are used interchangeably, the temperature T (in Kelvin) must be stated. However, the characterization of a single material is not very useful as most TECs as seen in Figure 2 possess both n-type and p-type materials. Thus, the merit is typically given as:

$$ZT = \frac{(S_p - S_n)^2 T}{(\rho_n \kappa_n)^{1/2} - (\rho_p \kappa_p)^{1/2}} \quad (4)$$

As with most devices, we may wish to determine the performance or efficiency depending on the usage. Using what we understand from the Seebeck effect causing a thermocouple to act as a power generation device, the efficiency of a thermoelectric couple η, is given by:

$$\eta = \frac{W}{Q_H} = \frac{\frac{V_{OC}^2}{R}\frac{m}{(m+1)}}{\frac{A}{L}\int_{T_c}^{T_h}\kappa(T)dT + IT_h S(T_h) - \frac{1}{2}I^2 R} \quad (5)$$

where V_{oc} is the open-circuit voltage applied to the system, m is the ratio of the load resistance RL/R, the internal resistance, $S(T_h)$ is the Seebeck coefficient at the hot side of the generator, A is the cross sectional area of single pellet, and L is its length. For simplification, we ignore the Thomson effect, a reversable effect that explains the property whereby the metal wires (Figure 1) themselves heat and cool in response to the changing temperature gradients between the two junctions. Simplification of this equation is performed by taking the following to be true:

$$R = \frac{1}{T_h - T_c}\frac{L}{A}\int_{T_c}^{T_h} \rho(T)dT \quad (6)$$

$$I = \frac{V_{OC}}{R(1+m)} \quad (7)$$

$$V_{OC} = \int_{T_c}^{T_h} S(T)dT \quad (8)$$

which yields:

$$\eta = \frac{\frac{m}{1+m}}{\frac{1+m}{Z(T_h - T_c)} + \frac{S(T_h)T_h}{\int_{T_c}^{T_h} S(T)dT} - \frac{1}{2(1+m)}} \quad (9)$$

To maximize the efficiency, take the derivate $\frac{d\eta}{dm}$, which yields the optimal setup m_{opt}:

$$m_{OPT} = \sqrt{1 + Z\Delta T\left(\frac{S(T_h)T_h}{\int_{T_c}^{T_h} S(T)dT} - \frac{1}{2}\right)} \quad (10)$$

Define $\frac{S(T_h)T_h}{\int_{T_c}^{T_h} S(T)dT}$ as a nondimensional intensity factor of the Thomson effect, which we will take as 1, which reduces (10) to:

$$m_{OPT} = \sqrt{1 + ZT_M} \quad (11)$$

where T_M is mean value of the hot and cold temperatures. Substituting (11) into (9) with our assumptions yields

$$\eta = \eta_C \frac{m_{OPT} - 1}{m_{OPT} + (\frac{T_C}{T_H})} \quad (12)$$

It is important to note that the efficiency would approach the Carnot efficiency $\eta_C = \frac{T_h - T_c}{T_h}$ as ZT_M approaches infinity. While there is neither a thermodynamic nor theoretical reason for a practical limit to exist, this upper value for most materials is $ZT \approx 1$ [4]. However, recent super lattice, mixed composition materials have been able to achieve a ZT of up to 2.4 [5]. The coefficient of performance ϕ (for refrigeration) can also be solved using the same assumptions:

$$\phi = \frac{Q_C}{W} = \frac{IT_C S(T_C) - \frac{A}{L}\int_{T_c}^{T_h} \kappa(T)dT - \frac{1}{2}I^2R}{\frac{V_{OC}^2}{R}\frac{m}{(m+1)}} = \frac{T_c}{T_h - T_c}\frac{m_{OPT} - (\frac{T_H}{T_C})}{m_{OPT} + 1} \quad (13)$$

Equation (13) approaches $\frac{T_c}{T_h - T_c}$ as the maximum theoretical efficiency for a TEC as m_{OPT} approaches infinity. This expression will act as the efficiency limit approached by the devices that I will test.

Background of Project

Over the following months I will perform analyses on two sets of TECs, henceforth named TECA and TECB. Initial studies have indicated that TECAs have been failing, resulting in the devices "opening" during standard operating conditions in the OCBs. As a result, the group will be testing TECs from another manufacture (TECB) to determine whether this issue can be resolved. Prior to my contribution to the project, characterization curves and failure analysis studies have been performed on the TECAs. My group found that the TECAs were operational during light-current-voltage (LIV) curve tracing before and after extreme –120% I_{OP} testing condition for 24 or fewer hours— testing conditions to cool laser temperatures to 25°C.

However, when the TECAs were installed in the OCBs, rather than maintaining the temperature of the lasers to 25°C, the lasers remained unregulated. TECA's inputs and outputs were also reading close to 0 current although proper operation dictated 1-2 amps. This led the team to surmise that the internal structure of the TECs was being compromised during operation, resulting in an increase in resistance. Four TECAs were subsequently sent to a third-party for failure analysis. Initial inspections found that there were neither external nor radiological abnormalities that could have resulted in the failures of the devices. However, upon de-lidding, de-soldering, and retesting the TECAs outside of their packaging, fluctuations in resistance were found which confirmed the issues during SNL's testing. Scanning electron microscopy (SEM) imaging found horizontal fractures. As seen in Figure 3, these fractures were located close to the Bismuth Telluride (Bi_2Te_3) / Nickel (Ni) interface. It was explained that the consistent location of these fractures near their individual element terminations, where varied CTE valued materials resided, indicated that thermal fatigue played a role in the failure of the thermoelectric coolers. These fractures created higher-than-typical resistances, which in turn caused even more localized heating and subsequent cracking.

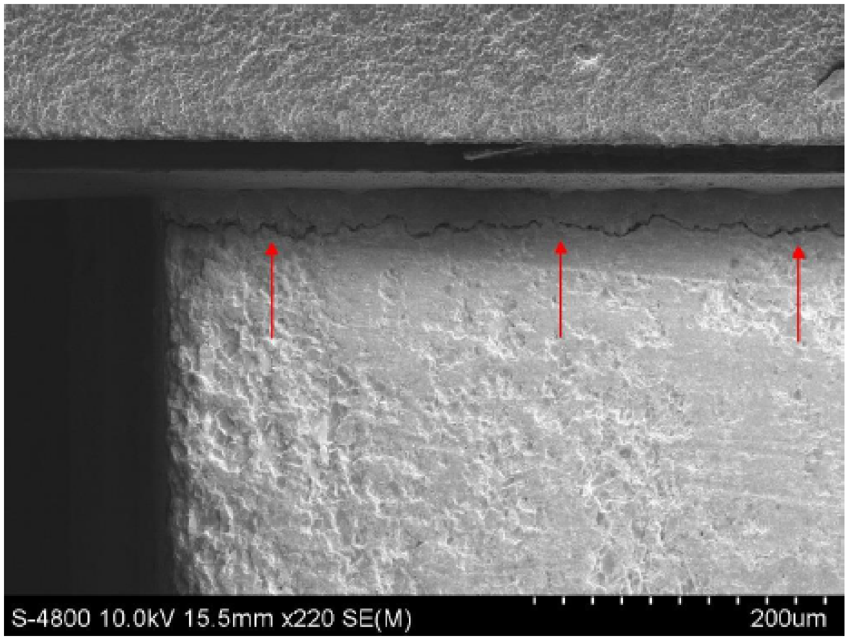

Fig. 3. Close-up SEM image of the cracked Peltier element leg

These cracks typically occur when there is a significant discrepancy between the coefficients of thermal expansion (CTE) across materials [6].

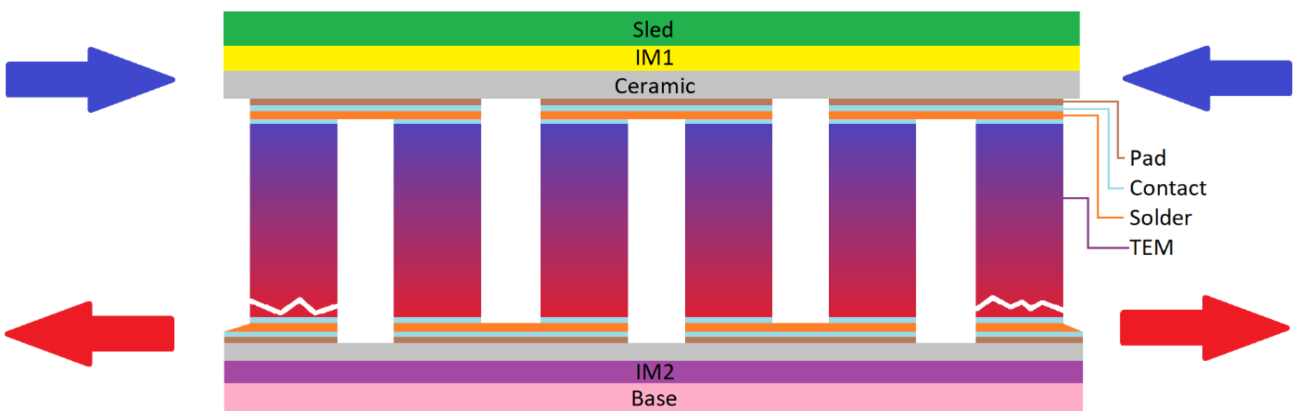

Fig. 4. Diagram of TECA device translated from EDS analysis illustrating cracking

While the initial failure analysis led the team in the right direction, a large concern was raised over the method of testing. The packages needed to be reflowed in order to separate them from the package. This could have introduced the solder voiding seen in the TECAs, which would undoubtedly reduce the overall efficiency of the device. A second round of tests conducted on the TECA parts applied more aggressive testing by thermal cycling the TECAs ten times between -40°C and 52°C over a 4-hour soak. They tested for failures by tracing their LIV curves. Of the 12 TECAs tested, 3 failed. One failed TECA and one functional TECA were cross-sectioned and captured using energy-dispersive X-ray spectroscopy (EDS) and SEM again. The former confirmed the stack-up composition (Table 1, Figure 4) and the latter provided detailed imaging of the cracking that occurred in the device (Figure 5). Cutting open the packages eliminated any possible reflowing issue with the solder but could have introduced the possibility of cracks being created along the TE material during the process. It was also noted that even without reflowing, the voids were still present in the cross section (Figure 5).

TABLE 1. CTE DATA FOR TECA

Label	*Material*	*CTE (ppm/°C)*
IM1	77.2Sn-20In-2.8Ag	28.0
Ceramic	AlNi	4.5
Pad	Cu	17.0
Contact	Ni	13.3
Solder	AuSn	16.0
TEM	Bi_2Te_3	14-21
IM2	96.5Sn-3.0Ag-0.5Cu	23.5

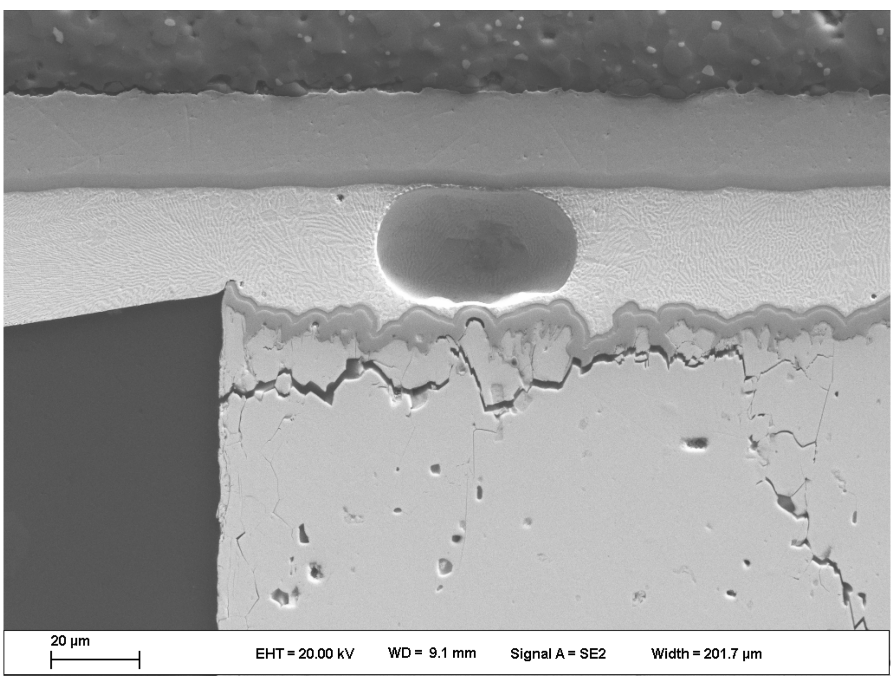

Fig. 5. SEM capture following device failure

Initially I suspected that a discrepancy between the Aluminum Nitride ceramic material ($CTE_{Ceramic}$) and outer casing of the laser module (CTE_{Base}) and/or sled that carries laser's heat load (CTE_{Sled}) was a possible cause of this issue. The TECA devices came pre-tinned with an interface material (IM) that needed to be reflowed and sandwiched between the two materials. This material solder was confirmed to not be of issue and was widely used and accepted. Yet, studies have found that the thermal load attached to Peltier junction can cause extremely high levels of thermal stress, which might cause dislocations and cracks of the material layers [7-9]. Although the Cu pads and Bi_2Te_3 pellets may vary in CTEs during operation (~ 12-18 and ~14-20 x 10^{E-6}, 1/K respectively [10,7]), the pad-contact-solder-contact-TEM stack up (Figure 4) provides enough cushion for drastic CTE changes. Moreover, the Ni contact that enhances solderability has been demonstrated to work well with BiTe TEMs to promote a strong mechanical structure [8]. However, the practical effects of TEC loading are typically not well documented. Instead, most papers assume zero loading on the cold side and a constant heat on the hot side [9]. Thus, examining the mechanical elements was where I began my initial investigation. Without knowing how the TECAs were soldered between the package and sled, these fractures may have been created during assembly. Thus, poor mounting techniques and/or incorrect CTE material selections were possible culprits for device cracking.

Unfortunately, due to time constraints, the packaging and sled material could not be changed. However, after the TECA's were sent to the laser packaging manufacturer, it was deemed that poor mounting techniques were involved in the process. Since then, several changes have been made as to how the laser package is mounted on the OCB. Specifically, a flatness specification was qualified, the pins on the laser packages were cut to the right lengths, a new design introduced flushed mounted tapped holes, the torque was reduced for the fasteners, and the laser mounting pad was changed to a Bergquist material. Nevertheless, the TECs were still exhibiting failures. Upon inspection of the failed TECs, it was found that even the working devices were exhibiting stress fractures.

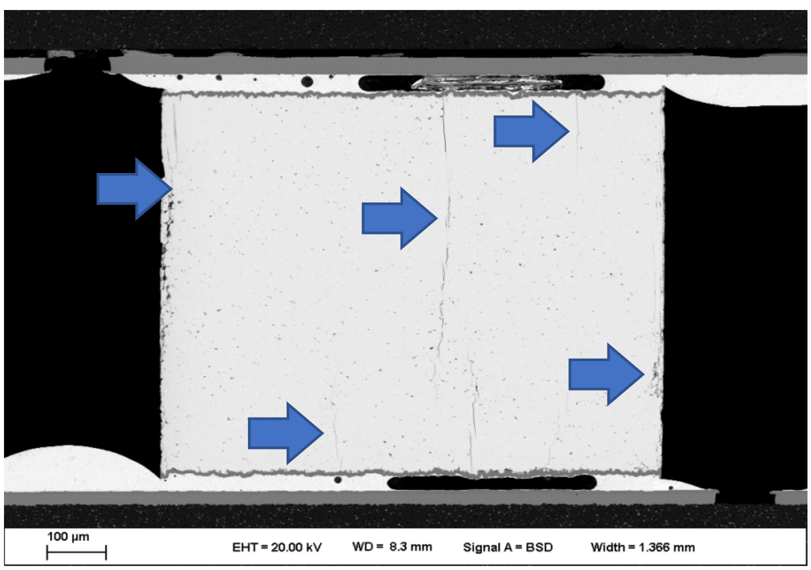

Fig. 6. Unmounted TEC SEM imaging

With only manufacturing defects as the culprit, two unmounted TECs were taken to be SEM imaged. The metallographic cross-sections indicated microfractures along the pellets (Figure 6). X-ray imaging of the unmounted TECAs was also performed which illustrated the large number of voids within the solder (Figure 7). These images confirmed a few important points:

1. Destructive SEM imaging was not the cause of the fractures
2. Voiding in the solder was present prior to even testing
3. The TECAs were objectively poorly manufactured

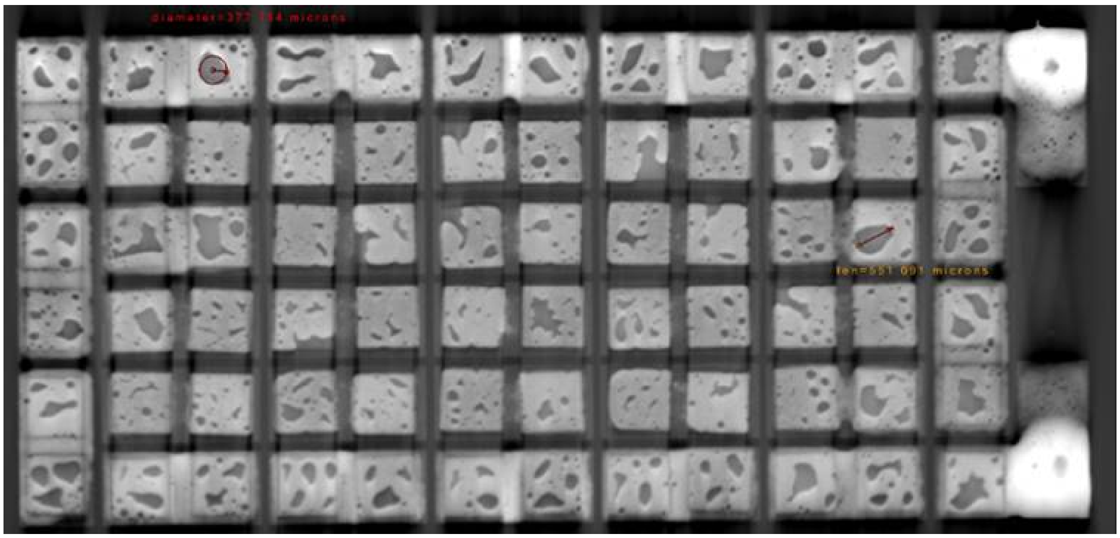

Fig. 7. X-ray imaging of unmounted TECAs

Current Progress of Project

Most of the time spent on this project has been invested in catching up on existing work performed for the study. I have worked with another member of the group to compose a test plan that will be carried out in the next months. This plan will be carried out for both sets of TECs (TECA and TECB) to determine if our thermal cycling testing conform to the tests conducted by other groups at Sandia. This will also be used a comparison study between the two TECs.

Terms and definitions

- Delta T (ΔT) – with no external heat to be absorbed, the device reaches its maximum rated ΔT. This is difference between temperature of T_H and T_C.
- Heat pumping capacity (Q_c) – once the cold side reaches the temperature of the heat sink, the TE cooler reaches its Q_{max}. This is amount of heat that the TEC can pump from the "cold" side.

- U_{max} – DC voltage needed to reach greatest ΔT. Although one would expect that this is the max voltage rating, increasing the voltage above the U_{max} instead decreases the ΔT because the power dissipation I^2R elevates the temperature, and this diminishes ΔT.
- I_{max} – DC current level that will produce the greatest ΔT
- Alternating Current Resistance (ACR) – The resistance of TEC's are unable to be measured using DC current because a ΔT will be produced across the module resulting in a Seebeck voltage that opposes the applied voltage. If read using ohmmeter, the resulting resistance will be higher than what is truly across the device. By applying an AC current, the polity will change every half-cycle and the Seebeck voltage will be diminished.
- Time constant (τ) - shows in very simple words the "TEC cooling rate" - the time TEC requires from switching on to a reach the stable cooling mode level [11].
- Figure-of-merit (Z) – derivation discussed in "Qualification of Thermoelectric Performance". Measurement of the "goodness" of TEC

Test Plan

A DX4085 Z-meter from TEC Microsystems has been ordered to aid in characterizing the TECA's in lab. It can measure the ACR, figure-of-merit (Z), and time-constant τ. For the first batch of tests, five unmounted TECA's will be tested. Below is a table explaining the meaning behind each reading. The TECs will be evaluated before and after impact tests are conducted. This far, impact tests will consist of thermal cycling according to each manufacturer's max temperature ratings.

TABLE 2. TEST CONDITIONS FOR UNMOUNTED TEC

Reasons of Defect	AC Resistance **ACR**	Figure-of-Merit **Z**	Time Constant **τ**	Comment
Metal junctions detachment	~ const	~ const	↑	τ ~ const @ low current
Confused p-n pellets polarity	~ const	↓	↑	
Thermal Contact between Pellet Side Wall and Solder Meniscus	~ const	↓	↓	
Thermal and Electric Contact of Pellet Wall and Solder Meniscus	↓	~ const	↓	
TEC Pellets Short Circuit	↓	↓	↓	
Two-stage TEC: confused stage polarity	~ const	~ const	↓	τ twice lower to nominal value

Reasons of Defect	AC Resistance **ACR**	Figure-of-Merit **Z**	Time Constant **τ**	Comment
TE material Degradation	↑	↓	~ const	

Test Procedures

Before the testing occurs, the TECs shall be labeled with unique serial numbers. The general procedure for the testing of the TEC is as follows:

1. Record the TEC Parameters (ACR, Z, τ) before any test condition is applied to the TEC. Record both the parameters at the current ambient temperature and the 27°C reference temperature. These are the beginning of life TEC parameters.
    a. Turn on Z-meter by pressing the top red button shortly
    b. Connect leads as close to the contact pins of the TECs as possible
    c. Place temperature sensor near TEC
    d. Confirm that the current reading is at 80mA, and the measuring time is 120 seconds
    e. Press green Start button and wait until yellow progress bar is complete
    f. Record ACR, Z, T, dTMax
    g. Press Mode once and record ambient temperature and corresponding ACR
    h. Pres Mode twice to return to main screen
    i. Repeat steps d-g until all TECs characterized
2. For each test condition,
    a. Record the TEC Parameters (ACR, Z, τ) before any test condition is applied to the TEC. Record both the parameters at the current ambient temperature and the 27°C reference temperature. These are the beginning of test TEC parameters.
    b. Apply the test condition to the TEC, which is documented in the Test Condition sections.
    c. Record the TEC Parameters (ACR, Z, τ) after the test condition is applied to the TEC. Record both the parameters at the current ambient temperature and the 27°C reference temperature. These are the after-test (AT) TEC parameters.
    d. Calculate the percent change of the TEC parameters from the beginning of life (BOL) measurement and beginning of test (BOT) measurement.

$$\%\ Change\ BOL = \frac{Parameter_{AT} - Parameter_{BOL}}{Parameter_{BOL}} \tag{14}$$

$$\%\ Change\ BOT = \frac{Parameter_{AT} - Parameter_{BOT}}{Parameter_{BOT}} \tag{15}$$

    e. Verify the TEC parameters have not changed by more than the limits in Table 3. These limits were decided in accordance with Electronics Industry Standard Telcordia GR-468 (MIL-883).
    f. If TEC parameters have changed, identify a failure defect based on Table 2

TABLE 3. TEC PARAMETER LIMITS

TEC Parameter	Limit
ACR	±5% of beginning of life
Z	±5% of beginning of life
τ	±5% of beginning of life

Thermal cycling will be performed on the TECs to determine the impact of extreme temperatures on the devices. The procedure for performing this part is listed as follows:

1. Measure the beginning of test TEC parameters.
2. Program the temperature chamber with the temperature profile in Table 4
3. Load the temperature chamber with the TEC DUTs. Put the TEC DUTs on a metal plate.
4. Start the temperature profile on the temperature chamber.
5. Wait for the temperature profile to complete.
6. Take the TEC DUTs out of the temperature chamber.
7. Measure the after-test TEC parameters.
8. Repeat steps 3-6 until the TECs fail or 10 cycles have been completed
9. Verify the TEC parameters are within tolerance and identify any defects.

TECA and TECB IV curves have been obtained from their respective manufacturers under life cycle testing and will be used for reference by comparing the results of the Z-meter testing. They can be found in Appendices A and B.

TABLE 4. TEMPERATURE PROFILE FOR THERMAL CYCLING

Total Time (Minutes)	Temperature (°C)	Dwell Time (Minutes)	Ramp Time (°C/Min)	Ramp Time (Minutes)
0	25			
30	25	30		
57.5	80		2	27.5
117.5	80	60		
177.5	-40		2	60
237.5	-40	60		
270	25		2	32.5
300	25	30		

Summary and Remaining work

In summary, the TECAs are ready to be tested using the Z-meter before and after thermal cycling impacting. In the upcoming months, the TECBs will arrive, and I will be ready to test these using the same procedure. If any of the TECs fail, I will send them our failure analysis team to verify the location of failure. After comparing the two TECs I should be able to provide a recommendation on how to proceed with the devices.

Given the resources, I would also like to explore the effects of the different load materials (aluminum, copper, tungsten, etc.) on the thermo-mechanical stress of the TECs. Another interesting test would be modifying the mounting orientation (epoxy, compression mounting) to see if these options improve the reliability of the devices. Although out of the scope of my knowledge, an interesting project would be modeling the TECs using finite element analysis to predict the effects of the aforementioned changes on the structural integrity of the system.

References

1. A. Allen, Laser Focus World, vol. 33. March 1997.
2. T. M. Tritt and M. A. Subramanian, "Thermoelectric Materials, Phenomena, and Applications: A Birds Eye View," *MRS Bulletin*, vol. 31, no. 3, pp. 188–198, 2006.
3. G. Karapetyan, *Physics and Mechanics of New Materials and Their Applications*. Nova Science Publishers, Inc., 2013.
4. T. Tritt, "Thermoelectric Materials: Principles, Structure, Properties, and Applications," *Encyclopedia of Materials: Science and Technology*, pp. 1–11, 2002.
5. R. Venkatasubramanian, E. Siivola, T. Colpitts, and B. Oquinn, "Thin-film thermoelectric devices with high room-temperature figures of merit," *Nature*, vol. 413, no. 6856, pp. 597–602, 2001.
6. N. Cusack and P. Kendall, "The Absolute Scale of Thermoelectric Power at High Temperature," *Proceedings of the Physical Society*, vol. 72, no. 5, pp. 898–901, 1958.

Sandia National Laboratories is a multimission laboratory managed and operated by National Technology & Engineering Solutions of Sandia, LLC, a wholly owned subsidiary of Honeywell International Inc., for the U.S. Department of Energy's National Nuclear Security Administration under contract DE-NA0003525. SAND2019-XXXX X

7. W. Liu, Q. Jie, H. S. Kim, and Z. Ren, "Current progress and future challenges in thermoelectric power generation: From materials to devices," *Acta Materialia*, vol. 87, pp. 357–376, 2015.
8. R. He, G. Schierning, and K. Nielsch, "Thermoelectric Devices: Thermoelectric Devices: A Review of Devices, Architectures, and Contact Optimization (Adv. Mater. Technol. 4/2018)," *Advanced Materials Technologies*, vol. 3, no. 4, p. 1870016, 2018.
9. T. Gong, Y. Wu, L. Gao, L. Zhang, J. Li, and T. Ming, "Thermo-mechanical analysis on a compact thermoelectric cooler," *Energy*, vol. 172, pp. 1211–1224, 2019.
10. F. C. Nix and D. Macnair, "The Thermal Expansion of Pure Metals: Copper, Gold, Aluminum, Nickel, and Iron," *Physical Review*, vol. 60, no. 8, pp. 597–605, 1941.
11. "Z-Meters - Why do you need one if you ... - TEC Microsystems." [Online]. Available: https://tec-microsystems.com/products/z-meters-for-express-qc/z-meter---why-do-you-need-one.html. [Accessed: 22-Jun-2020].

Appendix A: TECA Curves

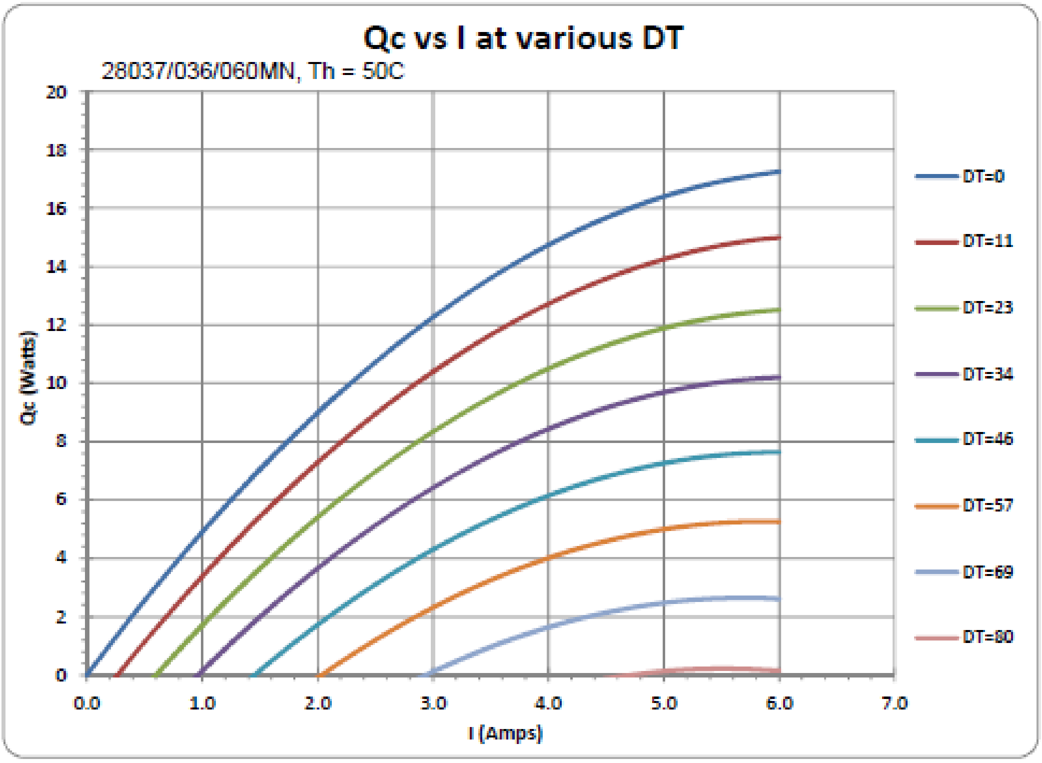

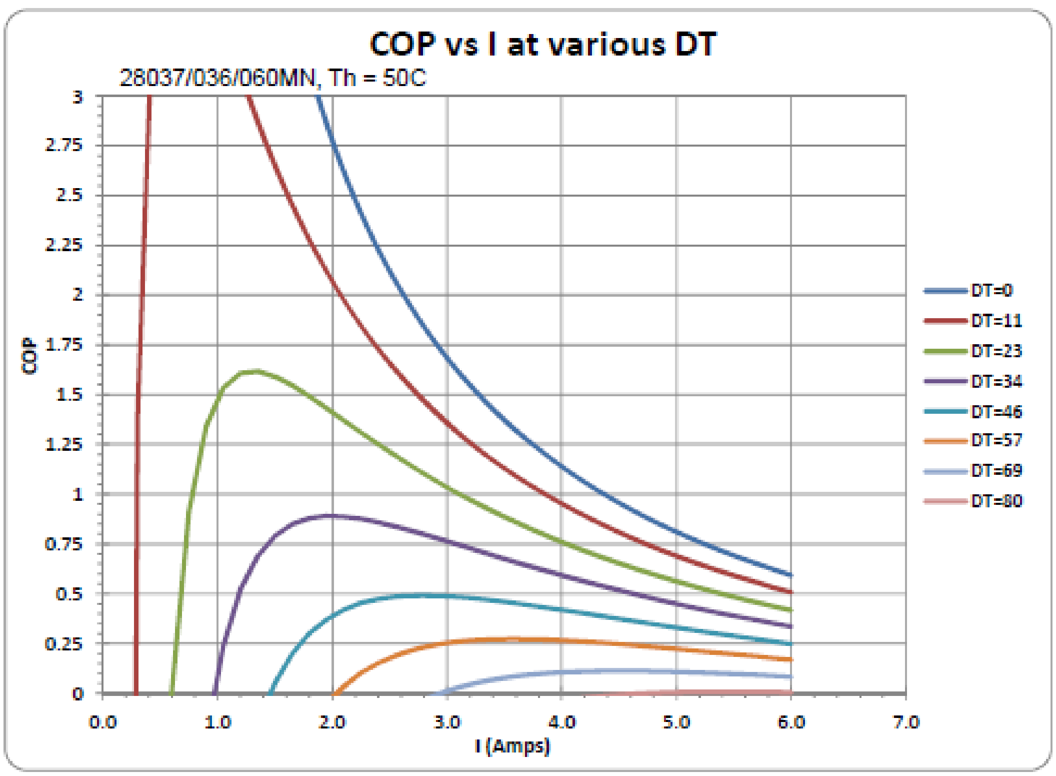

Sandia National Laboratories is a multimission laboratory managed and operated by National Technology & Engineering Solutions of Sandia, LLC, a wholly owned subsidiary of Honeywell International Inc., for the U.S. Department of Energy's National Nuclear Security Administration under contract DE-NA0003525. SAND2019-XXXX X

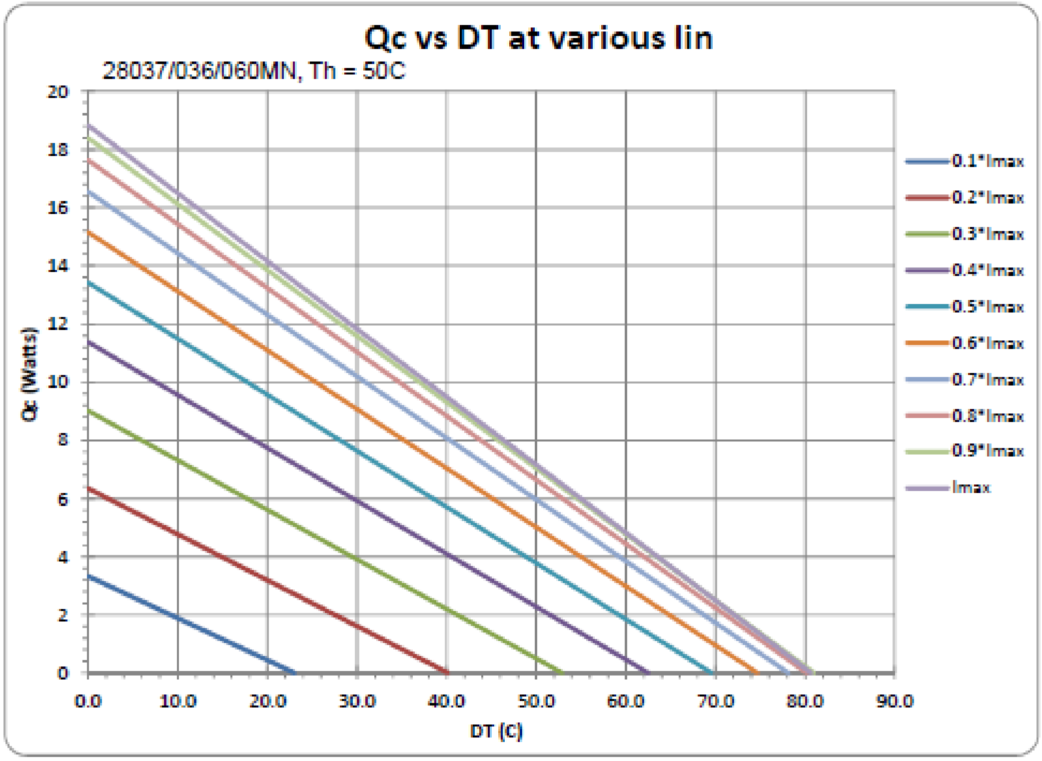

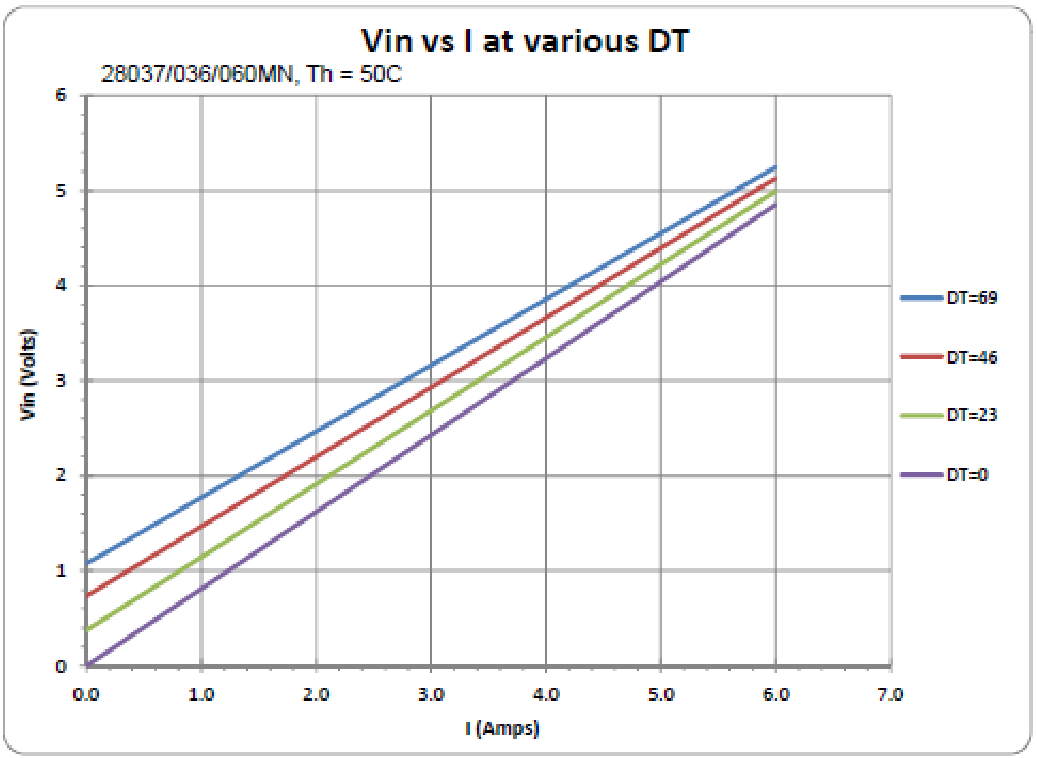

Sandia National Laboratories is a multimission laboratory managed and operated by National Technology & Engineering Solutions of Sandia, LLC, a wholly owned subsidiary of Honeywell International Inc., for the U.S. Department of Energy's National Nuclear Security Administration under contract DE-NA0003525. SAND2019-XXXX X

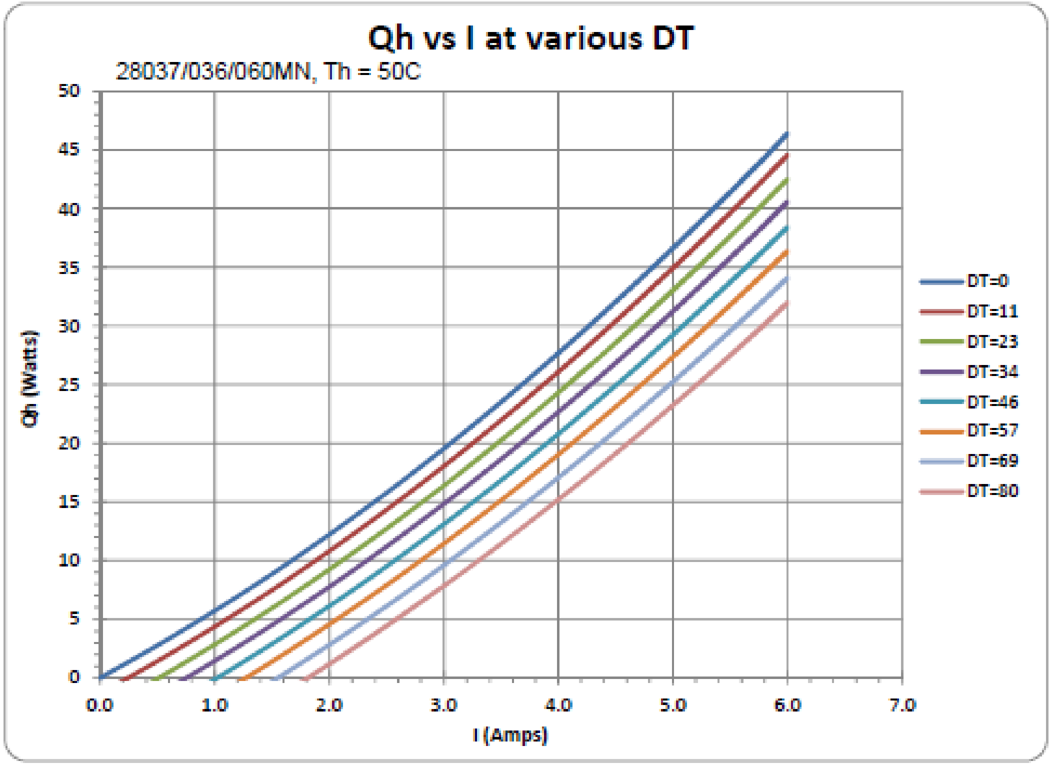

U.S. DEPARTMENT OF ENERGY NNSA National Nuclear Security Administration

Sandia National Laboratories is a multimission laboratory managed and operated by National Technology & Engineering Solutions of Sandia, LLC, a wholly owned subsidiary of Honeywell International Inc., for the U.S. Department of Energy's National Nuclear Security Administration under contract DE-NA0003525. SAND2019-XXXX X

Sandia National Laboratories

Appendix B: TECB Curves

@27°C, Vacuum	ΔTmax K	Qmax W	Imax A	Umax V
[redacted]	69	15.6	8.5	3.0

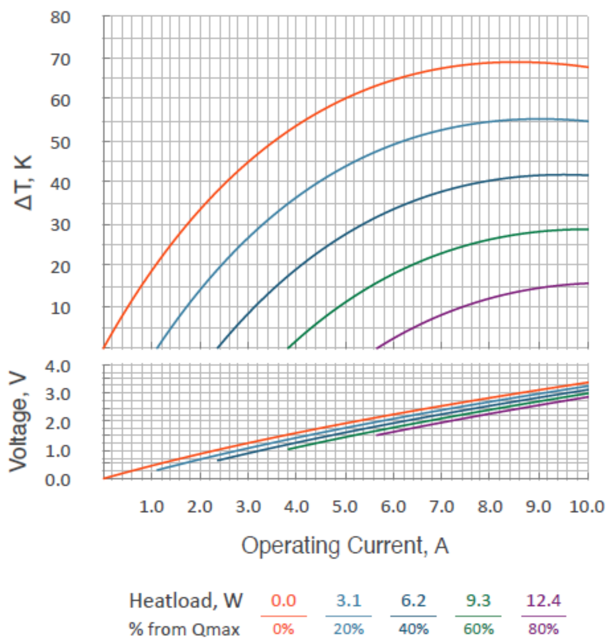

@50°C, Dry N2	ΔTmax K	Qmax W	Imax A	Umax V
[redacted]	75	17.0	8.5	3.3

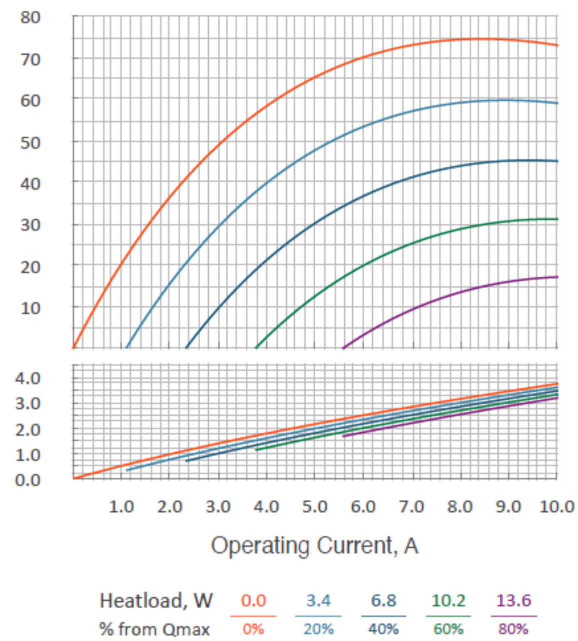

@75°C, Dry N2	ΔTmax K	Qmax W	Imax A	Umax V
[redacted]	80	18.4	8.3	3.6

@85°C, Dry N2	ΔTmax K	Qmax W	Imax A	Umax V
[redacted]	82	18.9	8.3	3.7

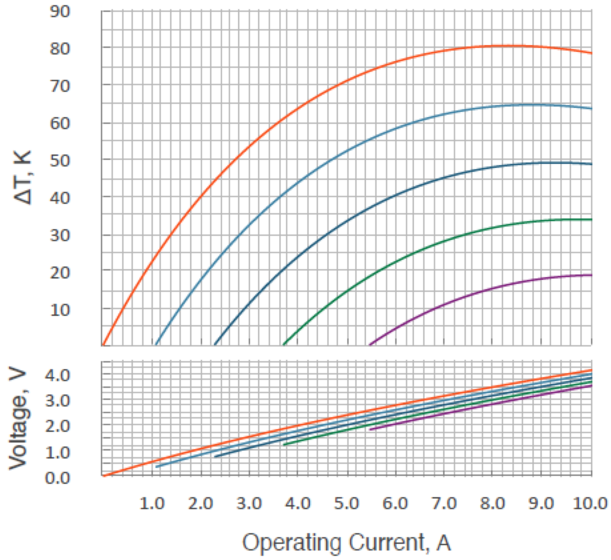

Heatload, W	0.0	3.7	7.3	11.0	14.7
% from Qmax	0%	20%	40%	60%	80%

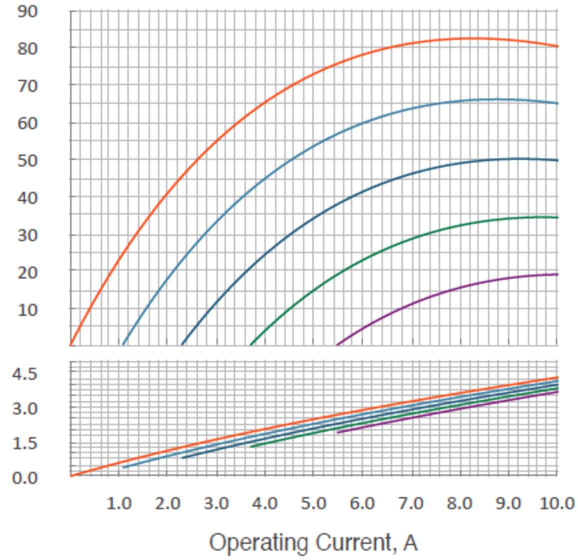

Heatload, W	0.0	3.8	7.5	11.3	15.1
% from Qmax	0%	20%	40%	60%	80%

Sandia National Laboratories is a multimission laboratory managed and operated by National Technology & Engineering Solutions of Sandia, LLC, a wholly owned subsidiary of Honeywell International Inc., for the U.S. Department of Energy's National Nuclear Security Administration under contract DE-NA0003525. SAND2019-XXXX X